

## Evolution of the inelastic x-ray scattering by $L$ and $M$ electrons into $K$ fluorescence in argon

J. Tulkki

Laboratory of Physics, Helsinki University of Technology, SF-02150 Espoo 15, Finland

(Received 31 January 1983)

The inelastic x-ray scattering by  $L$  and  $M$  electrons in the vicinity of the argon  $K$ -absorption edge is analyzed with the use of a generalization of the Kramers-Heisenberg formula. The theoretical cross section is given as a superposition of scattering probabilities to final  $(mp)^{-1}np$ ,  $n \geq 4$  discrete and  $(mp)^{-1}\epsilon p$  continuum states for  $m = 2$  and 3. The effect of the beamwidth on the spectrum of the scattered photons is discussed in detail. For a highly monochromatized beam the resolution is shown to increase by a factor of  $\Gamma_{1s}/\Gamma_{mp}$  as compared to  $K$  photoabsorption measurements. Our work demonstrates the possibility of using the inelastic resonance scattering for a detailed study of Rydberg and exciton states in the x-ray region.

### I. INTRODUCTION

In a recent Letter<sup>1</sup> we have analyzed the inelastic scattering by  $2p$  electrons in the vicinity of the Mn  $K$ -absorption edge in  $\text{KMnO}_4$ . Our theoretical differential cross section included both the effect of the beamwidth and the final-state lifetime. It was pointed out that for a beamwidth smaller than the widths of the  $(1s)^{-1}$  hole state one should obtain higher resolution for the scattering leading to bound final states as compared to the corresponding  $K$ -absorption spectrum. This resonance-fluorescence-like feature was not apparent in the experimental spectrum of Briand *et al.*<sup>2</sup> because of their relatively large bandwidth,  $\Gamma_b = 2.2$  eV as compared to  $\Gamma_{1s} = 1.16$  eV and  $\Gamma_{2p} = 0.33$  eV for Mn.<sup>3</sup>

New intense synchrotron radiation sources and multiple crystal monochromators will make x-ray Raman spectroscopy possible in the near future. In this work we discuss the overall features of this new "threshold spectroscopy" using the inelastic scattering by argon atoms as an example.  $K$  and  $L$  photoabsorption spectra of argon have been subject to intensive experimental studies.<sup>4-6</sup> The  $K$ -absorption spec-

trum has been analyzed by Watanabe<sup>7</sup> using a one-electron model. In his analysis only the two first Rydberg states with principal quantum numbers  $n = 4$  and  $n = 5$  were resolved. Recently, Deslattes *et al.*<sup>8</sup> have measured the  $K\beta$  emission spectrum of argon as a function of the beam energy to determine the threshold behavior of multivacancy processes. Related to this work it is shown that the high-resolution measurements of inelastic x-ray spectrum can give more accurate information on the discrete part of the threshold region than the corresponding absorption spectrum. We also demonstrate the half-width narrowing effect in the spectrum of the scattered photons as found by Eisenberger, Platzman, and Winick<sup>9</sup> in the case of Raman resonance scattering by  $L$  electrons at the Cu  $K$ -absorption edge.

### II. THEORY

In our earlier work<sup>1</sup> we have shown that the cross sections for the scattering leading to discrete  $(2p_j)^{-1}np$  ( $j = \frac{1}{2}, \frac{3}{2}$ ) and continuum  $(2p_j)^{-1}\epsilon p$  final states is given by

$$\frac{d\sigma(\omega_1)}{d\omega_2} = 2\pi r_0^2 \int_0^\infty \left( \frac{\omega_2}{\omega_1} \right) \frac{(\omega_{1s} - \omega_{2p_j}) g_{2p_j 1s}(\omega_{1s} + \omega) (dg_{1s}/d\omega)}{(\omega_{1s} + \omega - \omega_1)^2 + \Gamma_{1s}^2/4\hbar^2} \delta(\omega_1 - \omega_{2p_j} - \omega - \omega_2) d\omega, \quad (1)$$

where  $dg_{1s}/d\omega = g_{1snp} \delta(\omega + \omega_{np})$  for the discrete part. In Eq. (1) we have used the dipole approximation and included only the resonant part of the Kramers-Heisenberg formula. The resonant condition also limits the intermediate summation to  $(1s)^{-1}$  hole states. Our approach is based on the one-electron picture and consequently neglects post collision and unisotropic final channel interactions. Hence the differential cross section is isotropic. The oscillator strengths  $g_{2p_j 1s}$  of the  $K\alpha_2$  ( $j = \frac{1}{2}$ ) and  $K\alpha_1$  ( $j = \frac{3}{2}$ )

lines have been obtained from Scofield's<sup>10</sup> calculations.

In the discrete spectrum 15 Rydberg states were included corresponding to the principal quantum numbers  $4 \leq n \leq 18$ . The oscillator strengths  $g_{1snp}$  and the energies  $\hbar\omega_{np}$  have been evaluated from the quantum defect theory.<sup>11</sup> The energy of the  $4p$  Rydberg state was first calculated by the Dirac-Fock method. The calculated energy value  $E_{4p} = -2.87$  eV gives the defect  $\delta = 1.82$ . The oscillator strengths

were then defined by fitting the quantity  $g_{1np}(dn/d\omega_{np})$  to the zero-energy limit of the oscillator density ( $dg_{1s}/d\omega$ ), which is proportional to the  $K$ -edge value<sup>12</sup>  $\sigma_0^K$ , of the photoabsorption cross section. The oscillator density is given by  $dg_{1s}/d\omega = C\sigma_0^K f(\omega)$ , where  $C$  is a constant and where  $f(\omega)$  is an analytic function which accounts for the energy dependence of the density. The effect of the final-state lifetime was included by replacing the  $\delta$  function in Eq. (1) by a normalized Lorentzian density function with the half-width  $\Gamma_{2p}$ .<sup>13</sup> For the photon beam we used a Lorentzian distribution with an energy bandwidth  $\Gamma_b$  and with an exponential cutoff. Instead of Eq. (1) this results in a convolution, given by

$$\frac{d\sigma(\omega_1^0)}{d\omega_2} = \int_0^\infty \frac{d\sigma(\omega_1)}{d\omega_2} \left( \frac{dN_b}{d\omega_1} \right) d\omega_1, \quad (2)$$

where  $\omega_1^0$  corresponds to the maximum value of the beam distribution function  $dN_b/d\omega_1$ . In Eq. (2),  $\Gamma_{1s} = 0.68$  eV and  $\Gamma_{2p} = 0.127$  eV were used.<sup>3</sup> For the purpose of demonstration  $\Gamma_b$  was varied between 0.1 and 1.0 eV.

### III. RESULTS AND DISCUSSION

The behavior of the differential cross section is given in Fig. 1 for a bandwidth  $\Gamma_b = 0.1$  eV. Both continuum scattering, related to  $(2p_j)^{-1}\epsilon p$  ( $j = \frac{1}{2}, \frac{3}{2}$ ) final state and discrete scattering related to  $(2p_j)^{-1}np$  ( $4 \leq n \leq 18$ ) final states are shown. Above the  $1s$  ionization threshold,  $h\omega_{1s} = 3206.0$  eV, continuum spectra rapidly saturate to  $K\alpha_1$  and  $K\alpha_2$  fluorescence peaks at 2957.7 and 2955.6 eV, respectively. In contrast, the discrete features fade out. The peaks corresponding to  $n = 4, 5,$  and  $6$  are clearly resolved.

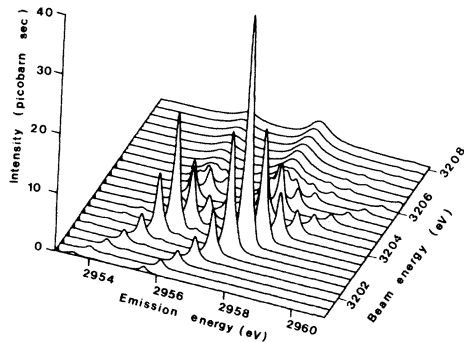


FIG. 1. Calculated differential cross section for x-ray Raman resonance scattering by argon atoms. The bandwidth  $\Gamma_b$  is 0.1 eV and the energy of the incoming beam is varied across the  $1s$  ionization threshold of argon. The final electronic states of the scattering atom or ion are  $(2p_j)^{-1}np$  ( $\epsilon p$ ) ( $j = \frac{1}{2}, \frac{3}{2}$ ).

Note that the peaks corresponding to  $(2p_{3/2})^{-1}np$  ( $6 \leq n \leq 18$ ) states overlap the peaks related to  $(2p_{1/2})^{-1}np$  ( $4 \leq n \leq 18$ ). Figure 2 presents the evolution of the  $(2p_{3/2})^{-1}np, \epsilon p$  cross section into  $K\alpha_1$  fluorescence for the bandwidths  $\Gamma_b = 0.1, 0.5,$  and  $1.0$  eV. The relative enhancement of the maxima of the discrete features as compared to the maximum of the fluorescence peak is prominent, especially in the case of  $\Gamma_b = 0.1$  eV as shown in detail in Fig. 3. In Fig. 4 the total cross sections are shown for  $\Gamma_b = 0.1$  and  $0.5$  eV. The total cross section is equal to the absorption cross section multiplied by the ratio of the radiative  $(1s)^{-1} \rightarrow (2p_{3/2})^{-1}$  transition probability to the total

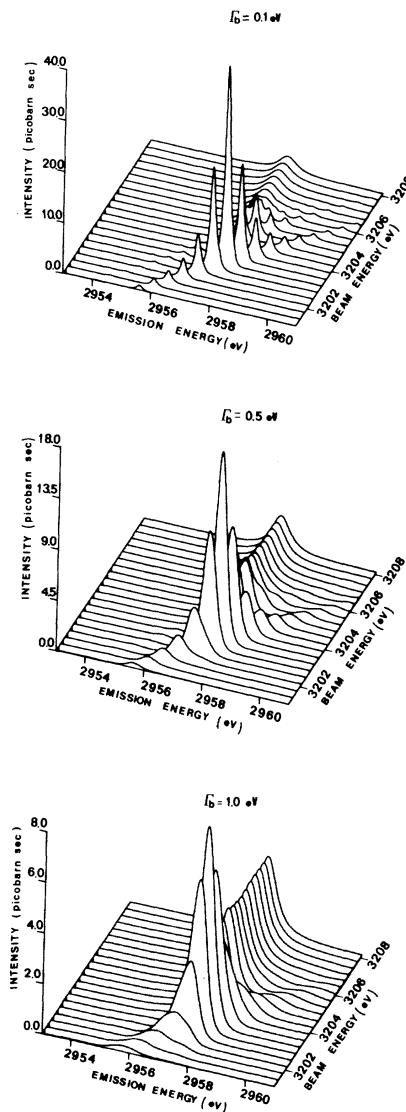


FIG. 2. Calculated differential cross sections for the bandwidths  $\Gamma_b = 0.1, 0.5,$  and  $1.0$  eV, respectively. Only the spectrum, corresponding to the  $(2p_{3/2})^{-1}np$  ( $\epsilon p$ ) final states, is shown.

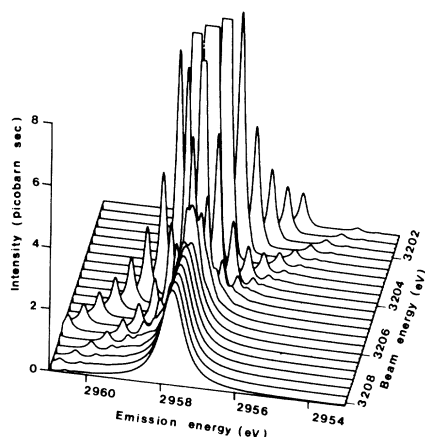


FIG. 3. Differential cross section for  $\Gamma_b = 0.1$  eV has been scaled by a factor of 5. The cutoff refers to 20% of the maximum in the spectrum.

decay rate of the  $(1s)^{-1}$  hole state. The absorption spectrum is a convolution of the beam-shape function and a Lorentz function with the  $\Gamma_{1s}$  half-width. The small difference in the total cross sections of Fig. 4 reflects the fact that in the case of  $\Gamma_b = 0.5$  eV we are already close to the theoretical resolution limit for the photoabsorption spectrum.

Figure 5 presents the inelastic scattering leading to  $(3p)^{-1}np, \epsilon p$  final state for  $\Gamma_b = 0.1$  eV. The final-state lifetime is practically infinite in this case and hence the resolution is limited only by the bandwidth. Recently, Deslattes *et al.*<sup>8</sup> have studied multivacancy effects in this spectrum. In Fig. 5 the multiple excited states of the type  $(1s)^{-1}(3l)^{-1}npl'$ ,  $(1s)^{-1}(3l)^{-1}np\epsilon'l$ , and  $(1s)^{-1}(3l)^{-1}\epsilon p\epsilon'l$  ( $l=0,1$ ) would cause a satellite structure situated mainly on the high-energy side of the discrete peaks and

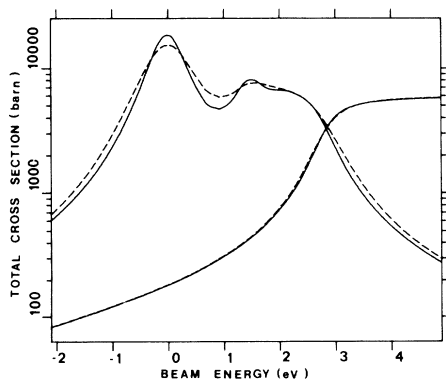


FIG. 4. Total cross sections for  $\Gamma_b = 0.1$  eV (solid line) and  $\Gamma_b = 0.5$  eV (dashed line) as a function of the difference between the beam energy and the  $1s \rightarrow 4p$  excitation energy. The peaks with the maximum at zero refer to the discrete part.

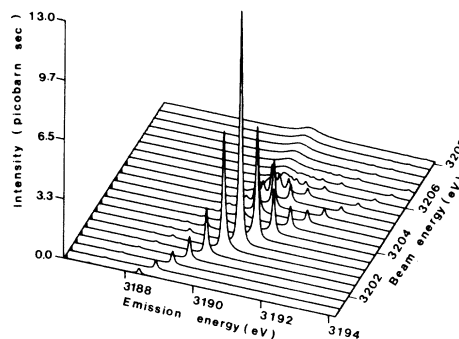


FIG. 5. Calculated differential cross section for scattering leading to  $(3p)^{-1}np(\epsilon p)$  final state of argon. The bandwidth  $\Gamma_b$  is 0.1 eV. The infinite final-state lifetime gives rise to an increased resolution as compared to the  $(2p)^{-1}$  case in Fig. 2.

fluorescence peak. The determination of the thresholds of the separate satellite groups may, however, be difficult for a number of reasons. As suggested by Deslattes *et al.*<sup>8</sup> the double excited  $(1s)^{-1}(3s)^{-1}nln'l'$  states are likely to decay by Coster-Kronig transitions before the  $1s$  hole is filled by radiative transition. As a function of the beam energy the behavior of the spectrum of the emitted photons pertaining to the doubly excited states is, however, different from that of singly and doubly ionized states. The difference in the total cross sections is as in Fig. 4, where the discrete contribution reaches a maximum in contrast to the continuum part which saturates. This may explain the maximum in the total  $K\beta^v$  satellite yield at the threshold, shown in Fig. 9 of Deslattes *et al.*<sup>8</sup>

The narrowing<sup>9</sup> of the half-width of the inelastic  $K\alpha$  peak slightly below the threshold can be seen in Fig. 6. This is due to the fact that on the high-

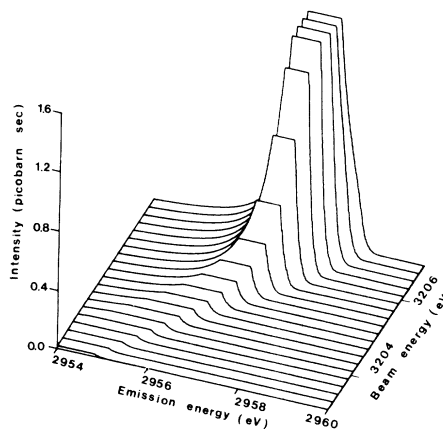


FIG. 6. Half-width narrowing effect in the continuum spectrum below the threshold. Each curve has been cut at the half-maximum value. The width of each cut is therefore equal to the half-width.

energy side of the fluorescence peak, the photon emission is forbidden by the energy conservation guaranteed by the final-state density. Hence for a narrow photon beam the shape of the high-energy side is characterized by the final-state lifetime. For broad beams no minimum would be observed.

In conclusion, we have shown that the inelastic scattering excited by a narrow photon beam can be used for high-resolution studies of exciton and Rydberg states in the x-ray region. The resolution of the spectrum of the scattered photons is limited by the lifetime of the final state. As compared to the corresponding absorption spectrum, the resolution is increased by a factor of  $\Gamma_{1s}/\Gamma_{2p_j}$  in the scattering leading to  $(2p_j)^{-1}np$  final state. In the case of argon the resolution for scattering leading to  $(3p_j)^{-1}np$  final state is solely limited by the bandwidth  $\Gamma_b$ . It is also

suggested that the "threshold spectroscopic" approach would lead to new possibilities regarding symmetry studies of exciton states. According to our earlier approach,<sup>14</sup> the angular distribution of emitted photons could be used to determine the symmetry of exciton states which are not separated in photoabsorption spectroscopy. This would provide valuable complementary information about the chemical environment of the scattering atom.

#### ACKNOWLEDGMENTS

I would like to thank Professor T. Åberg for valuable discussions and critical reading of the manuscript. I am also grateful to Dr. R. D. Deslattes and his group for information concerning their experimental work.

<sup>1</sup>J. Tulkki and T. Åberg, *J. Phys. B* **15**, L435 (1982).

<sup>2</sup>J. P. Briand *et al.*, *Phys. Rev. Lett.* **46**, 1625 (1981).

<sup>3</sup>M. O. Krause and J. H. Oliver, *J. Phys. Chem. Ref. Data* **8**, 329 (1979).

<sup>4</sup>H. W. Schnopper, *Phys. Rev.* **131**, 2558 (1963).

<sup>5</sup>M. Nakamura *et al.*, *Phys. Rev. Lett.* **21**, 1303 (1968).

<sup>6</sup>R. D. Deslattes, *Phys. Rev.* **186**, 1 (1969).

<sup>7</sup>T. Watanabe, *Phys. Rev.* **139**, A1747 (1965).

<sup>8</sup>R. D. Deslattes, R. E. LaVilla, P. L. Cowan, and A. Henins, *Phys. Rev. A* **27**, 293 (1983).

<sup>9</sup>P. Eisenberger, P. M. Platzman, and H. Winick, *Phys. Rev. Lett.* **36**, 623 (1976).

<sup>10</sup>J. H. Scofield, *Phys. Rev. A* **9**, 1041 (1974).

<sup>11</sup>U. Fano and J. W. Cooper, *Rev. Mod. Phys.* **40**, 441 (1968).

<sup>12</sup>W. M. Veigele, *At. Data* **5**, 51 (1973).

<sup>13</sup>W. Heitler, *The Quantum Theory of Radiation* (Oxford, Clarendon, 1954), Sec. V.20.

<sup>14</sup>J. Tulkki and T. Åberg, *J. Phys. B* **13**, 3341 (1980).